The EMBO Journal (2007) 26, 1691–1701 | © 2007 European Molecular Biology Organization | All Rights Reserved 0261-4189/07
www.embojournal.org

THE EMBO JOURNAL

Role of *Arabidopsis* AGO6 in siRNA accumulation, DNA methylation and transcriptional gene silencing

Xianwu Zheng, Jianhua Zhu, Avnish Kapoor and Jian-Kang Zhu*

Department of Botany and Plant Sciences, University of California, CA, USA

Argonautes (AGOs) are conserved proteins that contain an RNA-binding PAZ domain and an RNase H-like PIWI domain. In *Arabidopsis*, except for AGO1, AGO4 and AGO7, the roles of seven other AGOs in gene silencing are not known. We found that a mutation in *AGO6* partially suppresses transcriptional gene silencing in the DNA demethylase mutant *ros1-1*. In *ago6-1ros1-1* plants, *RD29A* promoter short interfering RNAs (siRNAs) are less abundant, and cytosine methylation at both transgenic and endogenous *RD29A* promoters is reduced, compared to that in *ros1-1*. Interestingly, the *ago4-1* mutation has a stronger suppression of the transcriptional silencing phenotype of *ros1-1* mutant. Analysis of cytosine methylation at the endogenous *MEA-ISR*, *AtREP2* and *SIMPLEHAT2* loci revealed that the CpNpG and asymmetric methylation levels are lower in either of the *ago6-1* and *ago4-1* single mutants than those in the wild type, and the levels are the lowest in the *ago6-1ago4-1* double mutant. These results suggest that AGO6 is important for the accumulation of specific heterochromatin-related siRNAs, and for DNA methylation and transcriptional gene silencing, this function is partly redundant with AGO4.

The EMBO Journal (2007) **26,** 1691–1701. doi:10.1038/sj.emboj.7601603; Published online 1 March 2007
Subject Categories: chromatin & transcription; plant biology
Keywords: Argonaute; RNA-directed DNA methylation; silencing; small RNA

Introduction

Gene silencing occurs at the transcriptional and post-transcriptional levels (Baulcombe, 2004; Bender, 2004; Mello and Conte, 2004; Chan *et al*, 2005; Matzke and Birchler, 2005; Morris, 2005; Wassenegger, 2005). Post-transcriptional gene silencing (PTGS) involves microRNAs (miRNAs) and certain classes of short interfering RNAs (siRNAs) (Carrington and Ambros, 2003; Bartel, 2004; Baulcombe, 2004; He and Hannon, 2004; Tang, 2005). miRNAs are about ~21–22 nt in size and are processed by Dicer family of endonuclease III enzymes from longer precursor RNAs that can form stem-loop structures (Carrington and Ambros, 2003; Bartel, 2004). siRNAs are generated from long double-stranded RNAs (dsRNAs) by enzymes of the Dicer family (Baulcombe, 2004; Matzke and Birchler, 2005; Bouche *et al*, 2006; Moissiard and Voinnet, 2006). There are two major size classes of siRNAs, that is, ~21- and ~24-nt siRNAs (Brodersen and Voinnet, 2006). miRNAs and siRNAs are incorporated into RNA-induced silencing complex (RISC) and guide the complex to complementary mRNAs, causing translational inhibition or transcript cleavage (He and Hannon, 2004; Meister and Tuschl, 2004; Tang, 2005). siRNAs of the 24-nt size classes can also guide DNA methylation and histone methylation to cause transcriptional gene silencing (TGS) (Baulcombe, 2004; Bender, 2004; Mello and Conte, 2004; Chan *et al*, 2005; Matzke and Birchler, 2005; Morris, 2005).

The PAZ and PIWI domain-containing Argonaute (AGO) proteins are the catalytic engine of RISC in PTGS (He and Hannon, 2004; Meister and Tuschl, 2004). In TGS, AGO is also a key component of RNA-induced transcriptional silencing complex (Verdel and Moazed, 2005) or of a hypothetical complex responsible for RNA-directed DNA methylation (RdDM) (Chan *et al*, 2005; Matzke and Birchler, 2005). In *Schizosaccharomyces pombe*, a single AGO protein mediates both transcriptional and post-transcriptional silencing (Sigova *et al*, 2004). In *Caenorhabditis elegans*, mutants defective in a member of the AGO gene family, *RDE-1,* are strongly resistant to RNA interference (RNAi) (Tabara *et al*, 1999). Another PAZ/PIWI protein, PPW-1, is required for efficient germline RNAi (Tijsterman *et al*, 2002). Systematic analysis of AGO mutants in *C. elegans* showed that distinct AGOs act sequentially during RNAi (Yigit *et al*, 2006). In *Drosophila,* AGO2 is directly involved in RISC formation as 'Slicer' of the passenger strand of the siRNA duplex (Rand *et al*, 2005). AGO1, another member of the *Drosophila* AGO family, immunopurified from Schneider2 cells associates with miRNAs and cleaves target RNAs that are fully complementary to the miRNAs (Miyoshi *et al*, 2005). PIWI has been shown to be necessary for PTGS and some aspects of TGS (Pal-Bhadra *et al*, 2002). In humans, AGO2 (hAgo2) was shown to be responsible for target RNA cleavage ('Slicer') activity in RNAi (Meister *et al*, 2004). In mouse, AGO2 contributes 'Slicer' activity to RISC, providing the catalytic engine for RNAi (Liu *et al*, 2004).

In *Arabidopsis,* there are 10 predicted AGO proteins (Morel *et al*, 2002). AGO1 was first found as a regulator of *Arabidopsis* leaf development (Bohmert *et al*, 1998). AGO1 is also involved in PTGS and viral resistance (Morel *et al*, 2002; Zhang *et al*, 2006). It functions as an RNA slicer that selectively recruits miRNAs and some siRNAs (Vaucheret *et al*, 2004; Ronemus *et al*, 2006). AGO4 controls locus-specific siRNA accumulation and DNA methylation (Zilberman *et al*, 2003, 2004). Maintenance of the hetero-

*Corresponding author. Department of Botany and Plant Sciences, University of California, 2150 Batchelor Hall, University of California, Riverside, CA 92521, USA. Tel.: +1 951 827 7117; Fax: +1 951 827 4437; E-mail: jian-kang.zhu@ucr.edu

Received: 17 July 2006; accepted: 24 January 2007; published online: 1 March 2007

chromatic state involves locus-specific Pol IVa function followed by siRNA production and assembly of AGO4- and NRPD1b-containing silencing complex within nucleolar processing centers (Pontes *et al*, 2006). AGO4 interacts with the C-terminal domain of NRPD1b, and its stability depends on upstream factors that synthesize siRNAs (Li *et al*, 2006; Pontes *et al*, 2006). AGO4 can function at target loci through two distinct and separable mechanisms. First, AGO4 can recruit components that signal DNA methylation in a manner independent of its catalytic activity. Second, through the catalytic activity of AGO4, secondary siRNAs are generated to reinforce silencing (Qi *et al*, 2006). ZIPPY (AGO7) functions in the regulation of developmental timing and is needed for the production and/or stability of some *trans*-acting siRNAs (Hunter *et al*, 2003, 2006; Adenot *et al*, 2006; Fahlgren *et al*, 2006; Garcia *et al*, 2006). PINHEAD/ZWILLE (AGO10) plays a critical role in maintaining undifferentiated stem cells in the shoot apical meristem, but was found not to participate in PTGS (Moussian *et al*, 1998; Lynn *et al*, 1999; Morel *et al*, 2002). The functional roles of other AGO proteins in *Arabidopsis* remain to be determined.

In this study, we characterized a second site mutation that suppresses TGS in the Arabidopsis *ros1-1* mutant. ROS1 is a 5-methylcytosine DNA glycosylase/lyase required for preventing DNA hypermethylation. In *ros1* mutants, TGS occurs at the *RD29A-LUC* (firefly luciferase reporter gene driven by the stress-responsive *RD29A* promoter) transgene and the linked kanamycin -resistance gene *35S-NPTII* (neomycin phosphotransferase II driven by the CaMV 35S promoter), and at the endogenous *RD29A* gene. Both the transgene and endogenous *RD29A* promoters are hypermethylated, which may be triggered by siRNAs produced from the transgene *RD29A* promoter (Gong *et al*, 2002). The suppressor mutation can partially release TGS at both transgene and endogenous *RD29A* promoters, but not at the *35S-NPTII* transgene. In *ago6-1ros1-1* double mutant, the cytosine methylation levels at both transgenic and endogenous *RD29A* promoters are reduced, and the amount of siRNAs generated from *RD29A* promoter region is much less than in *ros1-1* plants. The suppressor mutation also reduces the levels of siRNAs and DNA methylation at some endogenous loci. The suppressor mutation was found to be in AGO6, a member of the AGO family. In addition, we found that the *ago4-1* mutation can have a more complete suppression of *ros1*, compared to *ago6-1*. DNA methylation analysis of several endogenous loci in the *ago4ago6* double mutant showed that the effect of the double mutant is stronger than either of the single mutants. Our results suggest that AGO6 has a partially redundant function with AGO4 in siRNA accumulation and in controlling DNA methylation and TGS at specific loci.

Results

Partial suppression of transgene and endogenous RD29A promoter transcriptional silencing in ros1-1 by the ago6-1 mutation

We screened for suppressors of *ros1-1* from a T-DNA-mutagenized population (Kapoor *et al*, 2005) based on the enhanced bioluminescence compared with that in *ros1-1* mutant. One of the suppressor mutants with increased bioluminescence (Figure 1A, C and D) was designated as *ago6-1*. The *ago6-1* mutation, however, did not release the TGS of *35S-NPTII* (Figure 1B), because the *ros1-1ago6-1* plants are kanamycin -sensitive. This is in contrast to the *rpa2* mutant (Kapoor *et al*, 2005), which can release the silencing of *35S-NPTII* but not the linked *RD29A-LUC* in the *ros1-1* mutant background. The results from *rpa2* mutant studies suggested that the TGS of 35S-*NPTII* in *ros1-1* mutant is not caused by siRNAs and is also not dependent on DNA methylation (Kapoor *et al*, 2005).

Northern blot analysis revealed that in *ros1-1ago6-1* double-mutant plants, the endogenous *RD29A* transcript accumulated to a level higher than in *ros1-1* but the level was not as high as in the wild-type (WT) plants, indicating that the suppression of the endogenous *RD29A* gene silencing in *ros1-1* is partial, as is the suppression of the *RD29A-LUC* transgene. However, the *ros1-1ago6-1* mutant did not accumulate any *NPTII* transcripts, which is consistent with the kanamycin-sensitive phenotype of these plants (Figure 1E), and suggests that there is no suppression of the *35S-NPTII* transgene gene silencing.

DNA methylation level at the RD29A promoter in ros1-1 is reduced by the ago6 -1 mutation

In *ros1-1* mutant plants, DNA hypermethylation in the promoter region of both the *RD29A-LUC* transgene and the endogenous *RD29A* gene causes TGS at the two loci (Gong *et al*, 2002). We hypothesized that, in *ros1-1ago6-1* plants, the *ago6-1* mutation suppresses the TGS in *ros1-1* probably by reducing the levels of DNA methylation at the promoter regions. Bisulfite sequencing was carried out to determine the DNA methylation levels at both the transgene and endogenous *RD29A* promoter regions. As shown in Figure 2A and B, and in Supplementary Figure 1A and B, DNA methylation levels at CpG, CpNpG and asymmetric sites of the transgene *RD29A* promoter were decreased in *ros1-1ago6-1* compared with those in *ros1-1* plants. At the endogenous *RD29A* promoter, a similar pattern of reduced methylation was found at CpG, CpNpG and asymmetric sites in the *ros1-1ago6-1* double mutant, compared to *ros1-1*. These results support our notion that decreased DNA methylation levels at the transgene and endogenous *RD29A* promoters resulted in the suppression of *ros1-1* by *ago6-1*.

The ago6-1 mutation reduces non-CpG methylation at specific endogenous loci

To determine whether the *ago6-1* mutation affects the DNA methylation of endogenous sequences not associated with the transgene, we analyzed DNA methylation at the *AtSN1* locus. First, a PCR-based method was used to determine whether *ago6-1* mutation affects DNA methylation level of the retrotransposon *AtSN1*. The abundance of PCR products amplified from *ago6-1* and *ros1-1ago6-1* plants was much lower than that from *ros1-1* and WT plants (Figure 2C), suggesting that the DNA methylation levels at the *AtSN1* locus in *ago6-1* and *ros1-1ago6-1* plants are lower than those in *ros1-1* and WT plants. To confirm the results obtained by the PCR-based method, we used bisulfite sequencing. Although CpG methylation levels were unchanged, *ago6-1* showed almost two-fold reduction in CpNpG and four-fold reduction in asymmetric methylation at the *AtSN1* locus (Figure 2D and Supplementary Figure 2A). We also carried out bisulfite sequencing of the 5S rDNA repeat. The results showed that there was no substantial reduction in CpG,

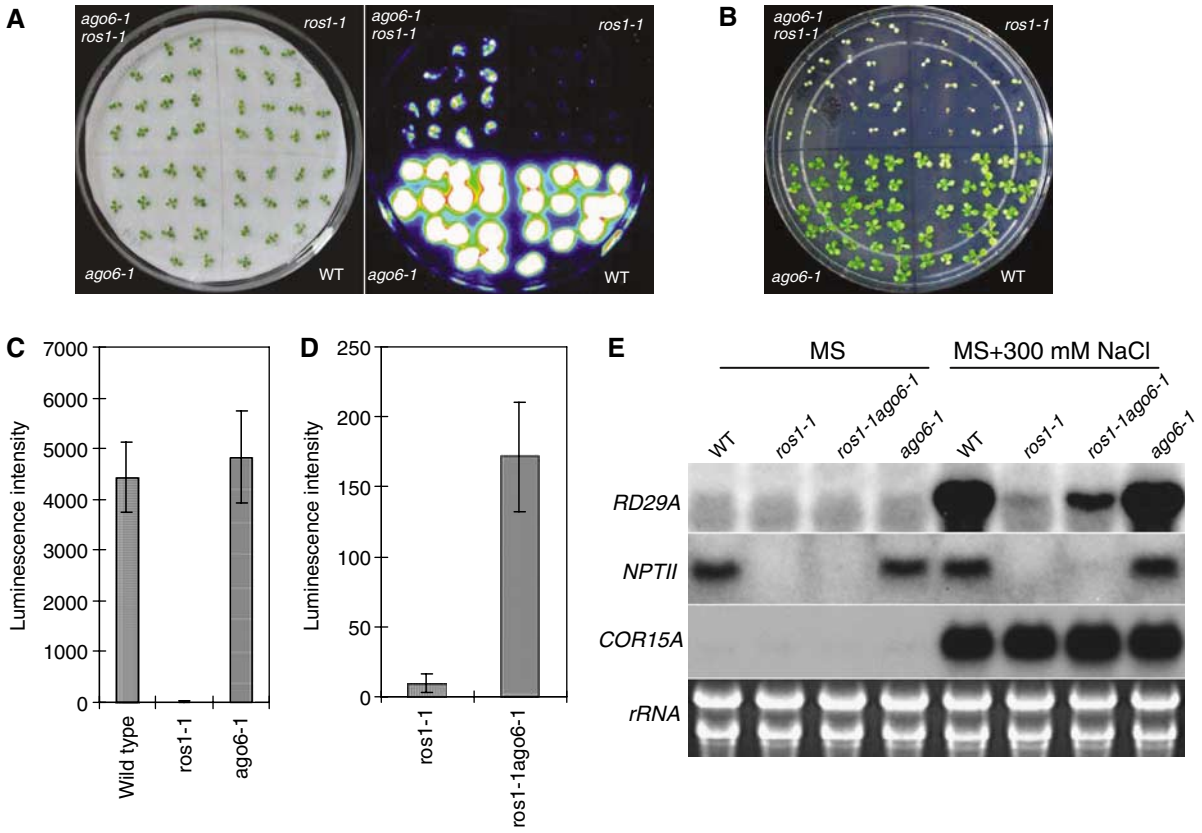

Figure 1 Partial suppression of *RD29A-LUC* and endogenous *RD29A* silencing but not of *35S-NPTII* silencing in *ros1* by *ago6*. (**A**) Luminescence image of WT, *ros1-1*, *ros1-1ago6-1* and *ago6-1*. Luminescence imaging was taken with 12-day-old seedlings treated with 300 mM NaCl for 5 h. (**B**) Phenotype of WT, *ros1-1*, *ros1-1ago6-1* and *ago6-1* plants plated on MS medium supplemented with kanamycin (50 μg/ml). (**C, D**) Quantification of the luminescence intensities of WT, *ros1-1*, *ros1-1ago6-1* and *ago6-1* plants treated with 300 mM NaCl for 5 h. (**E**) Northern blot analysis of the transcript levels of *NPT II*, endogenous *RD29A* and the stress-responsive control gene *COR15A* in WT, *ros1-1*, *ros1-1ago6-1* and *ago6-1*. WT, wild type of the C24 ecotype carrying a *LUCIFERASE* gene driven by the *RD29A* promoter (*C24 RD29A-LUC*).

CpNpG or asymmetric methylation in the *ago6-1* mutant (Figure 2E and Supplementary Figure 2B). These results suggest that *ago6* affects CpNpG and asymmetric methylation at some specific endogenous loci.

The ago6-1 mutation reduces the accumulation of heterochromatin-related siRNAs from transgene and endogenous loci

In *ros1-1* plants, DNA hypermethylation at the transgene and endogenous *RD29A* promoters may be triggered by siRNAs produced from the transgene promoter (Gong *et al*, 2002). It is possible that the reduced DNA methylation levels at the *RD29A* promoter regions in *ros1-1ago6-1* double mutant are a result of decreased accumulation or activity of the promoter siRNAs. Therefore, Northern blot analysis was carried out to assess the siRNA levels. The 24-nt siRNAs produced from the *RD29A* promoter were less abundant in *ago6-1* than that in the WT (Figure 3A), and similarly, the siRNA level was also less abundant in *ros1-1ago6-1* than that in *ros1-1* plants (Figure 3B). The siRNAs were absent in plants that do not contain the *RD29A-LUC* transgene, such as in Col-0, *dcl3-7*, *rdr2-1* and *ago6-2* plants (Figure 3A).

The accumulation pattern of several endogenous siRNAs was also investigated (Figure 3A). *AtSN1* and *MEA-ISR* siRNAs were detected in both *ago6-1* and *ago6-2*, but the levels were much lower than those in their respective WT backgrounds (Col-0 for *ago6-2*, and WT (C24 containing *RD29A-LUC*) for *ago6-1*). *AtREP2* and *SIMPLEHAT2* siRNA levels were also decreased in both *ago6-1* and *ago6-2* mutants compared to those in their respective WT. The levels of *siRNA1003* were not substantially different in *ago6-1* or *ago6-2*, compared to their respective WT controls. The *ago6* mutations also did not reduce the accumulation of siRNA02 (Figure 3A).

It has been shown that AGO1 is physically associated with miRNAs, but not with virus-derived siRNAs and 24-nt siRNAs involved in chromatin silencing (Baumberger and Baulcombe, 2005). We determined the levels of miRNAs to determine whether *ago6* mutations have any effect on miRNA accumulation. As shown in Figure 3A, there was no substantial reduction in miR165 or mi172 levels in any of the mutants compared to their respective WT controls. The above results show that AGO6 is partially required for the accumulation of certain 24-nt chromatin-related siRNAs.

The ago6-1 mutation does not affect PTGS caused by inverted repeat transgenes

PTGS of endogenous genes mediated by introduction of dsRNA was demonstrated in various organisms (Mello and Conte, 2004). To determine whether *ago6-1* affects siRNAs

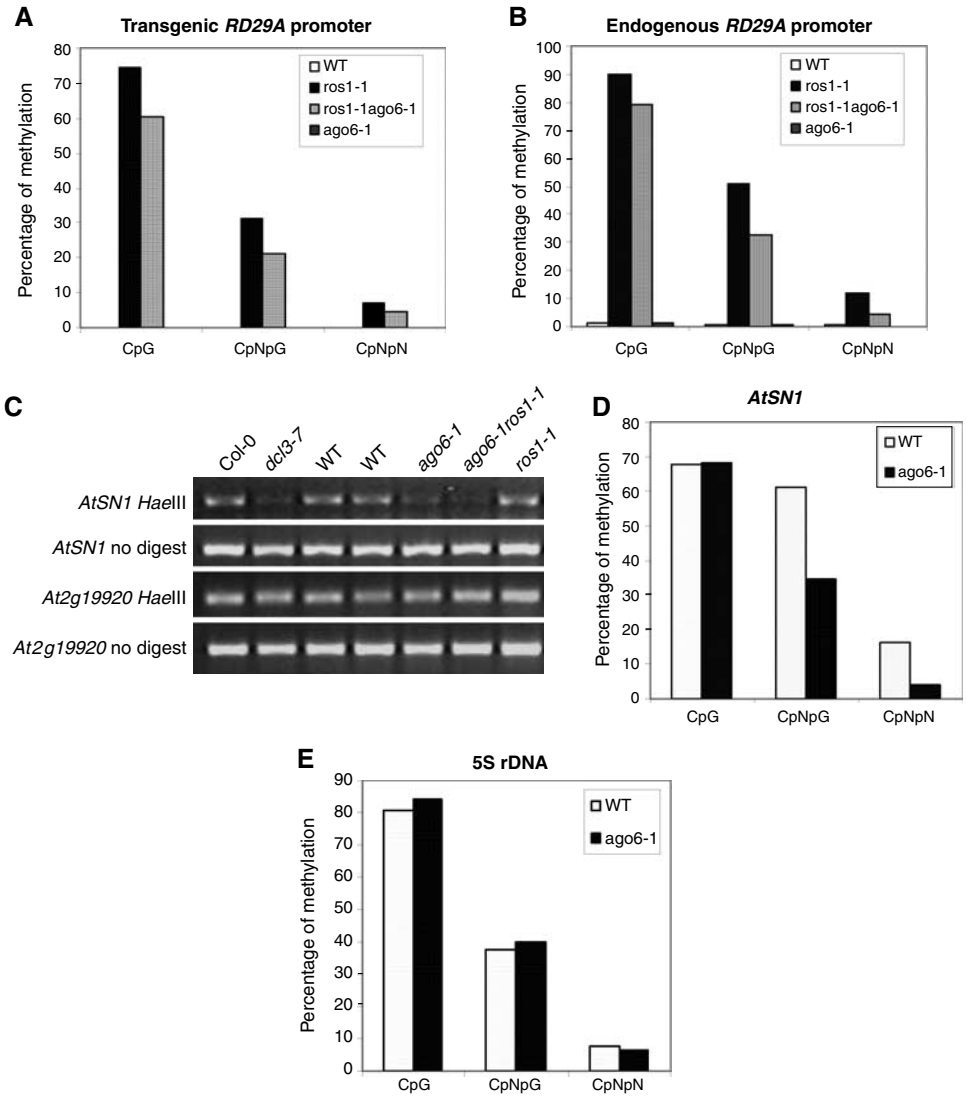

Figure 2 The effect of *AGO6* on DNA methylation levels. (**A**) DNA methylation levels (percent of methylated DNA) of transgenic *RD29A* promoter, and (**B**) DNA methylation levels of endogenous *RD29A* promoter in WT, *ros1-1*, *ros1-1ago6-1* and *ago6-1*. (**C**) *ago6-1* causes decreased *AtSN1* cytosine methylation. PCR was used to amplify a portion of the *AtSN1* retro-element. Undigested DNA and a gene lacking *Hae*III sites served as PCR controls. (**D, E**) DNA methylation levels at *AtSN1* and 5S rDNA in WT and *ago6-1*.

from hairpin constructs targeting mRNAs for cleavage, we crossed an inverted repeat construct of the *Arabidopsis MYB15* gene under the control of CaMV 35S promoter (Agarwal *et al*, 2006) to the *ago6-1* mutant background. Accumulation of siRNAs derived from the *MYB15* dsRNA construct and the transcript level of *MYB15* gene were detected by Northern blot and reverse transcription (RT)–PCR analyses, respectively. As shown in Figure 3C, the *MYB15* siRNA level in *ago6-1* plants was not substantially different from that in the WT. The result suggests that AGO6 is not required for the accumulation of siRNAs derived from PTGS inverted repeat constructs. Consistent with this, the expression of the target gene *MYB15* was silenced in *ago6-1* mutant, as in the WT, again indicating that AGO6 does not function in the RNAi pathway for PTGS.

Cloning and characterization of the AGO6 gene

To determine the T-DNA insertion site in the *ros1-1ago6-1* plants, thermal asymmetric interlaced PCR (TAIL-PCR) was carried out and an insertion was found in the 14th exon of the gene At2G32940, which is annotated as *AGO6*. This mutant allele was thus designated as *ago6-1* (Figure 4A). Another allele of *ago6* was obtained from the SALK T-DNA collection (Salk_031553), and was designated as *ago6-2* (Figure 4A). To determine whether the gene At2G32940 was responsible for the phenotype of TGS suppression of *ros1-1*, a cosegregation analysis was conducted. A cross was made between *ros1-1ago6-1* double mutant and *ros1-1* single mutant, and its F1 was then selfed to generate F2, from which 35 individual plants with enhanced bioluminescence were selected for PCR analysis to determine their genotype at the *AGO6* locus. The result showed that all of the 35 plants had a homozygous *ago6-1* insertion, suggesting that the *ago6-1* gene is responsible for the phenotype of enhanced luminescence in the *ros1-1ago6-1* plants.

To confirm further that At2G32940 is the correct gene, its genomic DNA including 1143 bp upstream of the initiation codon and 1533 bp downstream of the stop codon was cloned

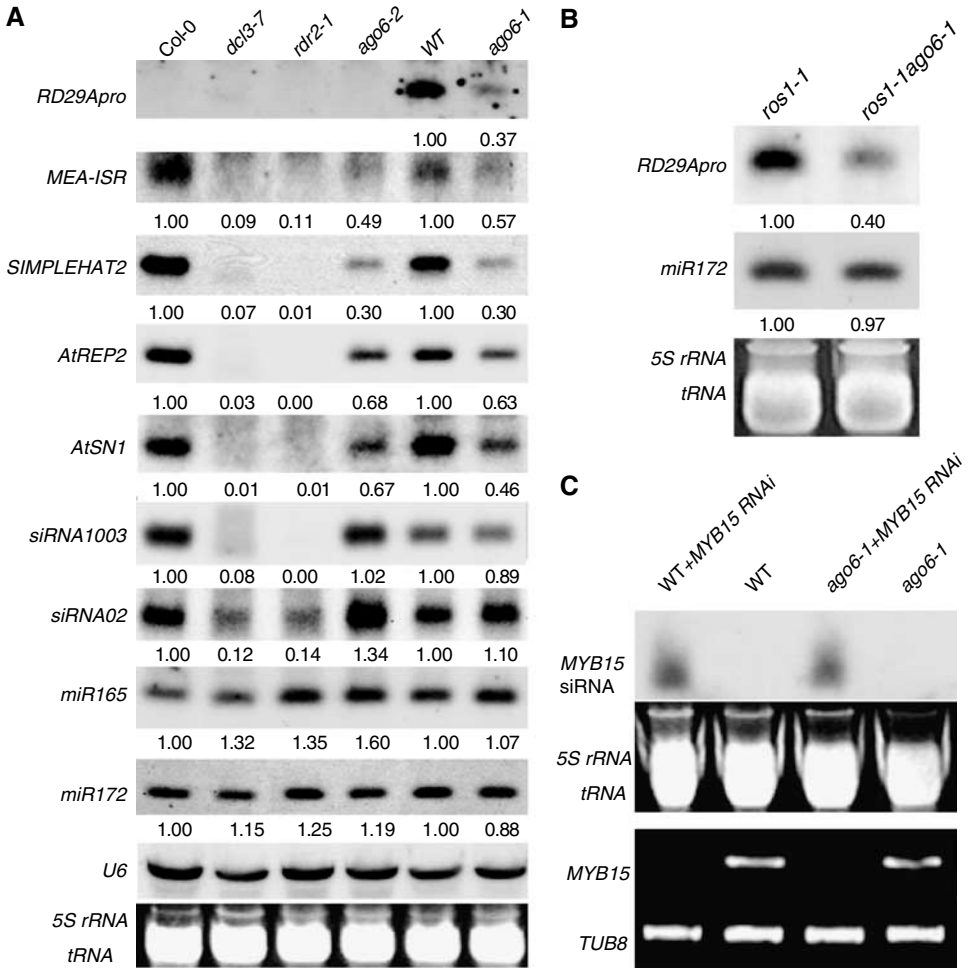

Figure 3 Effect of *ago6* on the accumulation of small RNAs. (**A**) Effect of *ago6* on the accumulation of siRNAs from the transgenic *RD29A* promoter, endogenous siRNAs and miRNAs. In addition to *ago6-1*, a SALK T-DNA insertion allele, *ago6-2* and its WT (Col-0) were also analyzed. snoRNA U6 and ethidium bromide-stained tRNA and rRNA bands served as loading controls. Relative levels of the small RNAs were calculated and shown below the small RNA bands. (**B**) The transgene *RD29A* promoter siRNA was less abundant in *ros1-1ago6-1* double compared with that in the *ros1-1* single mutant. (**C**) The effect of *ago6* on the accumulation of siRNAs from transgenic inverted repeat *MYB15* dsRNA. *MYB15* transcript levels were analyzed by RT–PCR.

by PCR amplification into the binary vector pCAMBIA1305.1, which was then introduced into *ros1-1ago6-1* plants by *Agrobacterium*-mediated transformation. T2 transgenic plants were subjected to phenotypic analysis. As shown in Figure 4B, a comparison of luminescence intensity of *ros1-1* single mutant, *ros1-1ago6-1* double mutant and *ros1-1ago6-1* double mutant expressing the *AGO6* transgene demonstrated that the AGO6 transgene construct restored the luminescence in *ros1-1ago6-1* to the level seen in *ros1-1*. Thus, the mutant was complemented, which confirms that *AGO6* is the correct gene (Figure 4B). We also used a PCR-based method to test the DNA methylation level at the *AtSN1* locus in *ros1-1*, *ros1-1ago6-1* and *ros1-1ago6-1* carrying the *AGO6* transgene. As shown in Figure 4C, in *ros1-1ago6-1* plants that contain the *AGO6* transgene, the DNA methylation level was restored to that in *ros1-1* plants, further confirming that *ago6* is responsible for the mutant phenotypes.

AGO6 encodes an 879-amino-acid protein that contains conserved PAZ and PIWI domains, characteristic of the AGO protein family. *Arabidopsis* contains 10 AGO proteins (Morel *et al*, 2002), and the available evidence suggests that each member may function differently. AGO1 and AGO4 were shown to participate in PTGS and TGS, respectively (Zilberman *et al*, 2003; Baumberger and Baulcombe, 2005). ZIPPY(AGO7) and PINHEAD/ZWILLE (AGO10) were found to have important roles in plant development (Moussian *et al*, 1998; Morel *et al*, 2002; Hunter *et al*, 2003). Phylogenetic analysis of full-length amino-acid sequences reveled that the 10 *Arabidopsis* AGO proteins fall into four clusters (Figure 4D). The AGO1, AGO5 and AGO10/PINHEAD/ZWILLE clade has high-sequence homologies with the human slicer AGO2, which was shown to target RNA for cleavage in the RNAi pathway (Meister *et al*, 2004). Indeed, recent studies showed that the *Arabidopsis* AGO1 is a bona fide Slicer (Baumberger and Baulcombe, 2005; Qi *et al*, 2005). AGO6 is in the same clade with AGO4, AGO8 and AGO9. AGO4 controls locus-specific siRNA accumulation and regulates DNA methylation (Zilberman *et al*, 2003, 2004). Our results, which that AGO6 also functions in siRNA accumulation and DNA methylation associated with TGS, is consistent with the phylogenetic clustering of AGO4 and AGO6. It is possible that the other two members of this cluster, AGO8 and

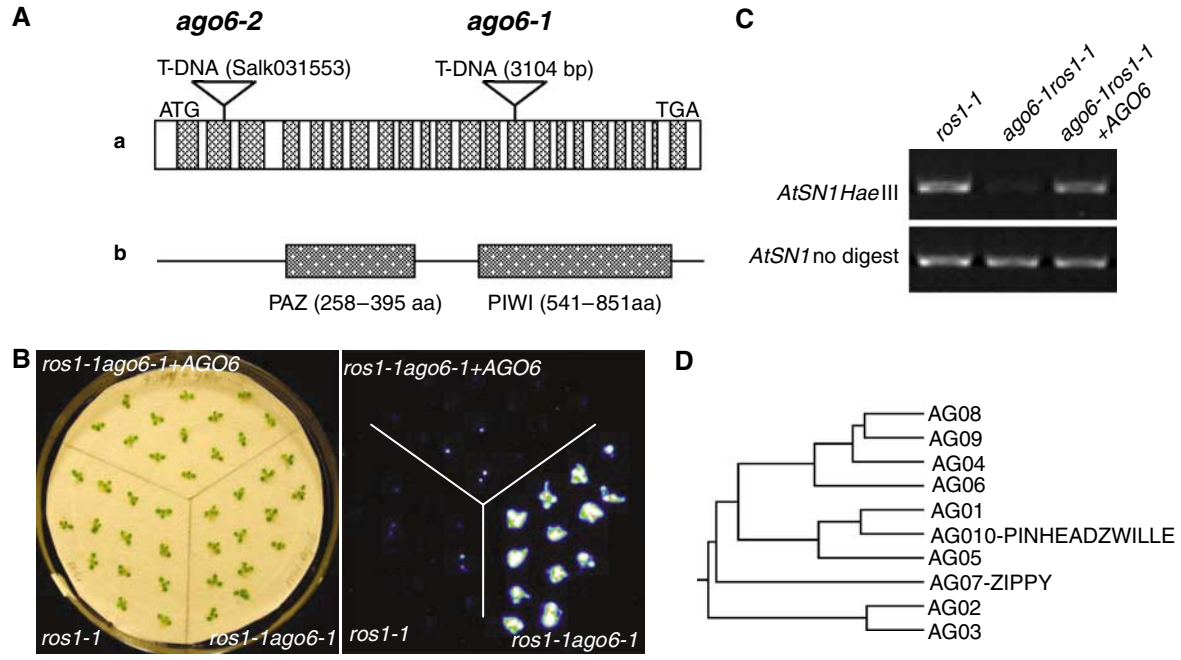

Figure 4 *AGO6* gene cloning and diagram of structure. (**A**) *AGO6* gene (At2G32940) structure. *AGO6* gene has a total of 22 exons and encodes a putative AGO protein containing a PAZ domain and a PIWI domain. *ago6-1* has a T-DNA insertion in the 14th exon, and *ago6-2* (a T-DNA line from the SALK collection) (Salk 031553) has an insertion in the second exon. (**B**) Complementation of *ago6-1* mutant. *ros1-1ago6-1* plants transformed with WT *AGO6* transgene were restored in the luminescence phenotype to that seen in *ros1-1*. (**C**) The molecular phenotype of *AtSN1* methylation in *ros1-1ago6-1* was restored after the *ros1-1ago6-1* double mutant was transformed with the WT *AGO6* gene. (**D**) Phylogenetic tree of the *Arabidopsis* AGO proteins using full-length amino-acid sequences. *AGO4, 6, 8* and *9* clustered together.

AGO9 also function in chromatin siRNA accumulation and DNA methylation.

To determine the subcellular localization of AGO6 protein, a translational fusion between yellow fluorescence protein (YFP) and the N terminus of AGO6 was carried out. YFP-AGO6 protein was found to be localized mainly in the nucleus and weakly outside the nuclear compartment (Figure 5A). A construct of *AGO6* genomic fragment containing an AGO6 C-terminal translational fusion to the MYC tag and driven by the endogenous *AGO6* promoter was transformed into *ros1-1ago6-1* double-mutant plants. This construct restored the *RD29A-LUC* silencing phenotype (data not shown). The T2 transgenic plants were subjected to immunostaining with the anti-MYC antibodies to confirm AGO6 protein localization. The result shows that the AGO6-MYC fusion protein was located in the nucleus (Figure 5Ba–c). In *ros1-1ago6-1* mutant plants without the *AGO6-MYC* transgene, there was no immunostaining in the nucleus (Figure 5Bd–f). There did not appear to be a clear immunostaining in the nucleolus (Figure 5B). This predominant nuclear localization of AGO6 is in line with its function in chromatin siRNA accumulation, DNA methylation and transcriptional silencing.

An *AGO6* promoter–GUS fusion was used to analyze *AGO6* gene expression pattern. As shown in Figure 5C, *AGO6* promoter–GUS expression was strong in roots, cotyledons and shoot meristematic region. The expression was weak in old and young leaves, and was not detectable in floral tissues.

Strong suppression of transcriptional silencing in ros1-1 by the ago4-1 mutation

As *AGO4* also controls locus-specific siRNA accumulation and DNA methylation (Zilberman *et al*, 2003, 2004), we wondered whether *ago4-1*, like *ago6-1*, may suppress transgene and endogenous *RD29A* promoter transcriptional silencing in *ros1-1*. We crossed *ago4-1* with *ros1-1* and subsequently obtained *ago4-1ros1-1* double-mutant plants. As shown in Figure 6A, *ros1-1ago4-1* double-mutant seedlings emitted strong bioluminescence compared to that from the *ros1-1* single mutant, indicating that *ago4-1* strongly suppresses the TGS of *RD29A-LUC* in *ros1-1* plants. We performed Northern analysis to determine if *ago4-1* can also suppress the silencing of the endogenous *RD29A* gene in *ros1-1*. The result shows that the transcript level of endogenous *RD29A* in the *ros1-1ago4-1* double mutant was nearly as high as that in WT plants (Figure 6B), indicating that *ago4-1* also suppresses the TGS of endogenous *RD29A* in *ros1-1*.

To determine whether the suppression effect of *ago4-1* is associated with changes in cytosine methylation, bisulfite sequencing was conducted at both transgene and endogenous *RD29A* promoters. We found that the CpG methylation level at transgene *RD29A* promoter was greatly reduced, and the methylation at CpNpG and asymmetric sites was almost lost in *ros1-1ago4-1* compared to that in *ros1-1* plants (Figure 6C and Supplementary Figure 3A). At the endogenous *RD29A* promoter, a similar pattern of reduced methylation at CpG, CpNpG and asymmetric sites was found in the *ros1-1ago4-1* double mutant (Figure 6D and Supplementary Figure 3B). These results suggest that the suppression of *ros1-1* by *ago4-1* was caused by decreased DNA methylation levels at the transgene and endogenous *RD29A* promoters.

AGO6 functions redundantly with AGO4

We crossed *ago6-1* and *ago4-1* plants, and generated an *ago6-1ago4-1* double mutant. DNA methylation levels at *MEA-ISR*,

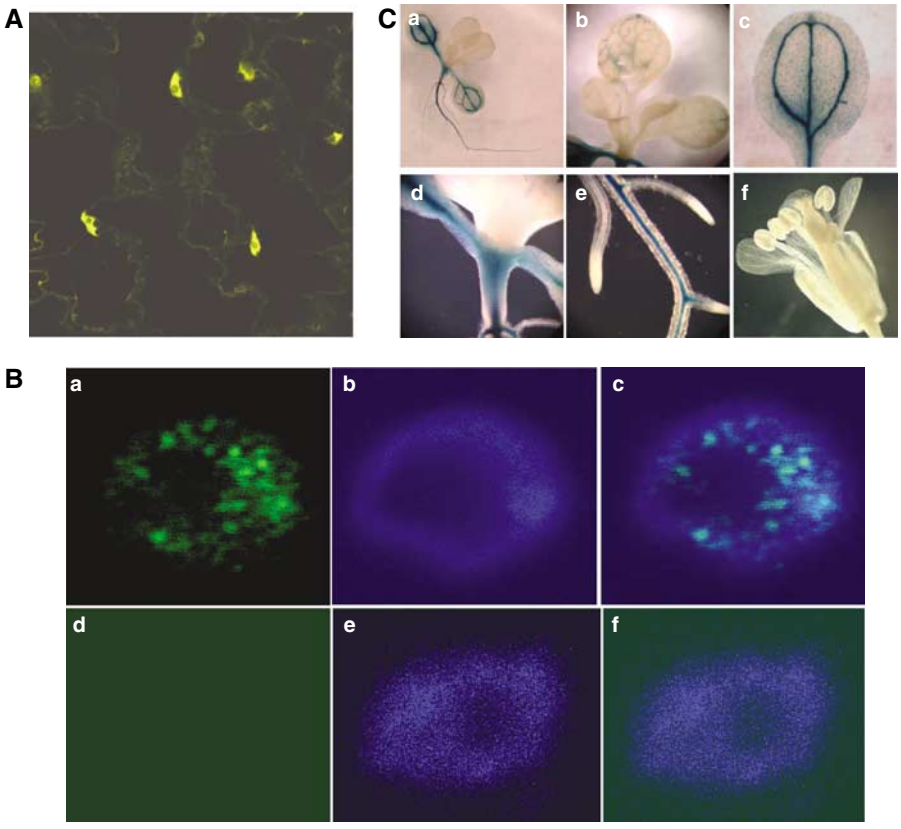

Figure 5 Subcellular localization of AGO6 protein and expression pattern of *AGO6* promoter-driven *GUS* reporter gene. (**A**) Expression of YFP–AGO6 translational fusion under the control of CaMV 35S promoter in the epidermal cells of *Arabidopsis*. YFP–AGO6 protein was mainly localized in nuclei, and weakly in the cytoplasm. (**B**) Subcellular localization of AGO6 protein detected by immunostaining. (a) Localization of AGO6-MYC. (b) Nucleus with DAPI staining. (c) Overlap of (a) and (b). (d), (e) and (f) are negative controls showing immunostaining of a nucleus from *ros1-1ago6-1* plant without the *AGO6-MYC* transgene. (**C**) *AGO6* promoter–GUS expression pattern. AGO6 was strongly expressed in roots (a, e) and cotyledons (a–d), very weakly in young leaves (a, b) and not detectable in floral tissues (f).

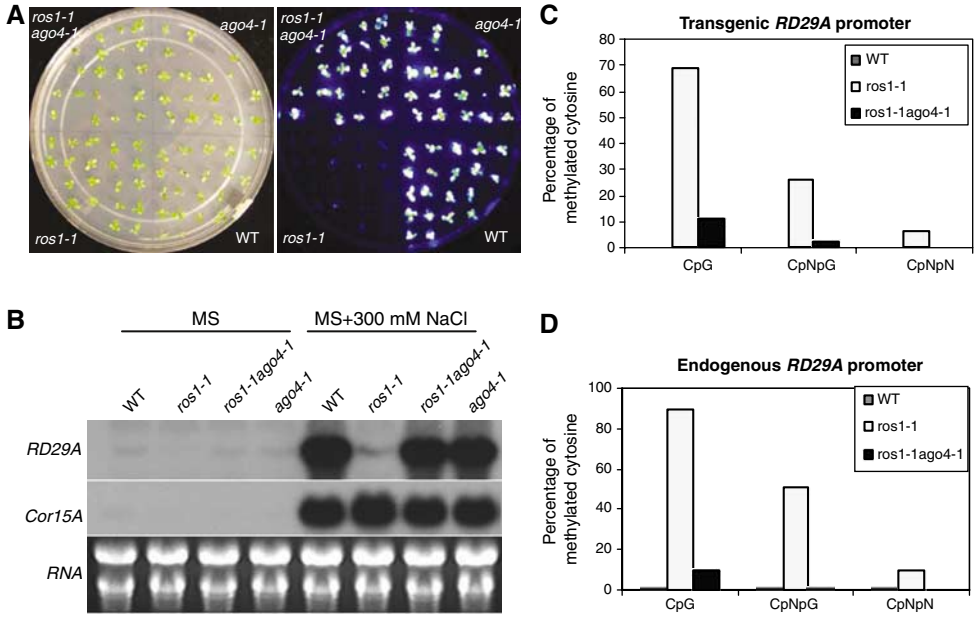

Figure 6 Strong suppression of *RD29A-LUC* and endogenous *RD29A* silencing in *ros1-1* by *ago4*. (**A**) Luminescence images of WT, *ros1-1*, *ros1-1ago4-1* and *ago4-1* seedlings. Luminescence images were taken with 12-day-old seedlings treated with 300 mM NaCl for 5 h. (**B**) Northern blot analysis of the transcript levels of endogenous *RD29A* and the stress-responsive control gene *COR15A* in WT, *ros1-1*, *ros1-1ago4-1* and *ago4-1*. (**C**) DNA methylation levels (percentage of methylated cytosine) of transgenic *RD29A* promoter, and (**D**) DNA methylation levels of endogenous *RD29A* promoter in WT, *ros1-1* and *ros1-1ago4-1*.

AtREP2, *SIMPLEHAT2* and *AtGP1* were analyzed in *ago6-1* and *ago4-1* single mutants, and in the *ago6-1ago4-1* double mutant. At the *MEA-ISR* (Figure 7Aa and Supplementary Figure 4A), *AtREP2* (Figure 7Ab and Supplementary Figure 4B) and *SIMPLEHAT2* (Figure 7Ac and Supplementary Figure 5A–C) loci, there were substantial decreases in the mutants in DNA methylation at CpNpG and asymmetric sites but not at CpG sites. The results show that both AGO6 and AGO4 are important for CpNpG and asymmetric but not CpG cytosine methylation at the *MEA-ISR*, *AtREP2* and *SIMPLEHAT2* loci. These results are consistent with the observation that both *ago6-1* (Figure 3A) and *ago4-1* (Qi *et al*, 2006) affect *MEA-ISR*, *AtREP2* and *SIMPLEHAT2* siRNAs. Importantly, the results show that in the *ago6-1ago4-1* double mutant, CpNpG and asymmetric cytosine methylation levels were even lower than those in *ago6-1* or *ago4-1* single mutant. In contrast, at the *AtGP1* locus the methylation level at CpG, CpNpG and asymmetric sites did not show substantial differences among WT, *ago6-1*, *ago4-1* and *ago6-1ago4-1* (Figure 7Ad and Supplementary Figure 5D), suggesting that *ago6-1* and *ago4-1* do not affect the DNA methylation level at this locus.

Northern blot analysis of *AtREP2* siRNAs in *ago4-1* and *ago6-1* single mutants and *ago4-1ago6-1* double mutant was carried out. As shown in Figure 7B, the *AtREP2* siRNA levels in *ago4-1*, *ago6-1* single mutants were lower than those in their respective WT controls. Furthermore, the *ATREP2* siRNA level in *ago4-1ago6-1* double mutant was lower than that in either *ago4-1* or *ago6-1* single mutant. The result is consistent with the effect of *ago4-1ago6-1* on the DNA methylation at the *AtREP2* locus. Taken together, these results suggest that the functions of *AGO6* and *AGO4* at some target loci are at least partly redundant.

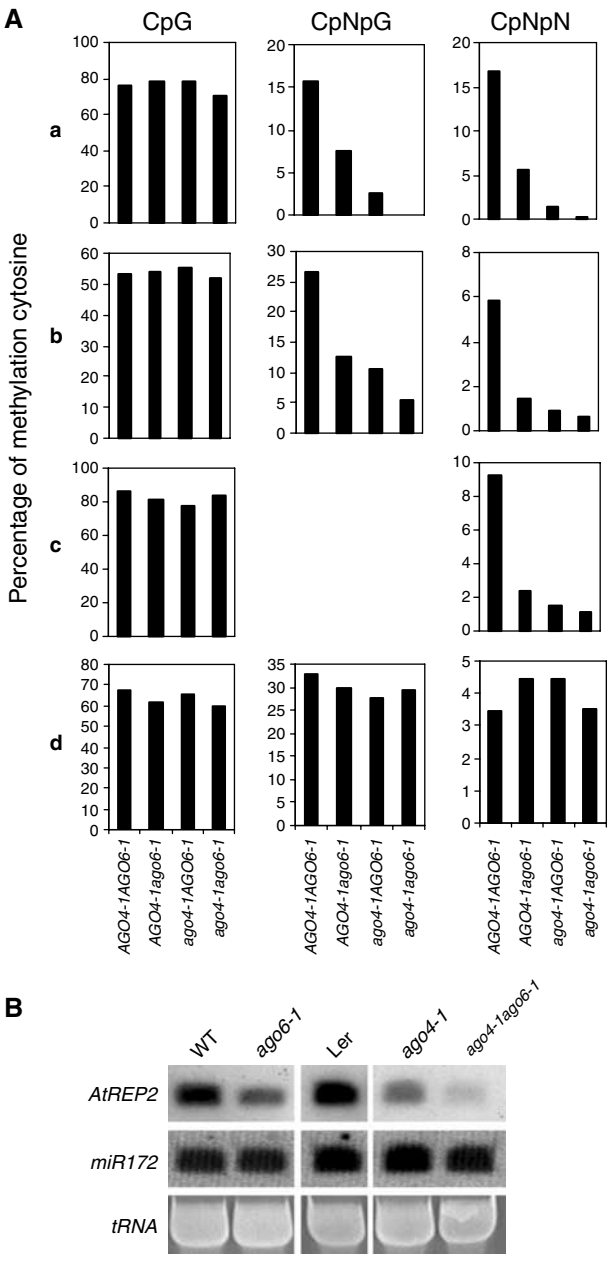

Figure 7 DNA methylation analysis at several endogenous loci in *AGO4-1AGO6-1*, *AGO4-1ago6-1*, *ago4-1AGO6-1* and *ago4-1ago6-1*. (**A**) CpG (left), CpNpG (middle) and CpNpN (right) methylation at the *MEA-ISR* (a), *AtREP2* (b), *SIMPLEHAT2* (c) and *AtGP1* (d) loci were analyzed by bisulfite sequencing. Methylation levels are shown by the percentage of methylated cytosine in all sequenced clones. Detailed bisulfite sequencing data are in Supplementary Figures. (**B**) Northern blot analysis of siRNAs at the *AtREP2* locus in *ago4-1*, *ago6-1* single mutants and *ago4-1ago6-1* double mutant. *miR172* was used as a control.

Discussion

In this study, we identified the *ago6-1* mutation as a suppressor of *ros1-1*. The *ago6* mutation partially releases TGS of transgenic *RD29A-LUC* and endogenous *RD29A* gene, but not of the *35S-NPTII* transgene caused by the ros1 mutation. Previously, we have reported that a mutation in the replication protein A2 suppresses the TGS of *35S-NPTII* but not *RD29A-LUC* or endogenous *RD29A*, in a DNA methylation-independent manner (Kapoor *et al*, 2005). Our study here further supports that the mechanism of silencing at *35S-NPTII* is different from that of silencing at the *RD29A* promoter.

Analyzing the DNA methylation pattern at both transgene and endogenous *RD29A* promoter regions revealed that in the *ros1-1ago6-1* double mutant the levels of CpG, CpNpG and asymmetric methylation were all decreased compared to those in *ros1-1* mutant. In addition, we found that *ago6-1* mutation reduces DNA methylation at endogenous targets such as *AtSN1*, *MEA-ISR*, *AtREP2* and *SIMPLEHAT2*, because the levels of CpNpG and asymmetric methylation were decreased in the *ago6-1* mutant. Interestingly, CpG methylation levels at these endogenous loci were not lower in the *ago6* mutant. Therefore, it seems that AGO6 is important for DNA methylation at all sequence context for some loci, but is only required for DNA methylation at non-CpG sites for some other loci.

siRNAs are believed to be the trigger for *de novo* DNA methylation in RdDM (Mello and Conte, 2004; Chan *et al*, 2005; Morris, 2005). Analysis of siRNA levels in *ago6-1* mutant showed that siRNAs from the transgenic *RD29A* promoter was substantially reduced. The *ago6-1* mutation also substantially decreased the levels of siRNAs from endogenous loci such as *AtSN1*, *MEA-ISR*, *AtREP2* and *SIMPLEHAT2*, but did not reduce *siRNA1003* and *siRNA02* levels. These results demonstrate an important role of AGO6 in the accumulation of specific chromatin-related siRNAs. In addition, our results suggest that AGO6 does not have a substantial effect on miRNAs and PTGS siRNAs from inverted

repeat transgenes. How AGO6 is involved in the accumulation of chromatin-related siRNAs remains an open question. It is possible that AGO6 functions in RdDM, and its role in siRNA accumulation is indirect and is perhaps through its effect on DNA methylation in a cycle of feed forward regulation involving transcription of methylated DNA to generate more siRNAs, similar to what has been proposed for AGO4 (Li *et al*, 2006; Pontes *et al*, 2006; Qi *et al*, 2006).

Arabidopsis has 10 members in the AGO family (Morel *et al*, 2002). AGO6 is in the same subfamily with AGO4, although within this subfamily AGO4 is more closely related in sequence to AGO8 and AGO9 than AGO6. AGO4 was first identified because of a partial suppression of epigenetic silencing at the *Superman* locus by *ago4* mutations (Zilberman *et al*, 2003). The *ago4* mutations decrease substantially non-CpG methylation but only affect slightly CpG methylation. The *ago4* mutations were shown to block the accumulation of *AtSN1,* 5S rDNA, *MEA-ISR, AtREP2* and *SIMPLEHAT2* siRNAs, but had no effect on siRNA02 (Zilberman *et al*, 2003, 2004; Li *et al*, 2006; Pontes *et al*, 2006; Qi *et al*, 2006). It seems that AGO6 and AGO4 have very similar or overlapping functions. Compared to *ago6*, the effect of the *ago4* mutations on siRNA accumulation and DNA methylation is stronger for some target loci such as the transgene and endogenous *RD29A* promoter regions and *MEA-ISR*. However, for some other target loci such as *AtREP2* and *SIMPLEHAT2*, the *ago6* and *ago4* mutations have comparable effects. It is possible that *ago6* may have a stronger effect than *ago4* on some as yet unidentified target loci. Analysis of DNA methylation in *ago4-1ago6-1* showed that non-CpG methylation at *MEA-ISR, AtREP2* and *SIMPLEHAT2* was lower in *ago4-1ago6-1* compared to *ago4-1* or *ago6-1* single mutant, suggesting that the two AGO proteins may have partially redundant functions. This notion is also supported by the much reduced *AtREP2* siRNAs in the *ago4-1ago6-1* double mutant compared to *ago4-1* or *ago6-1* single mutant. Clearly, much further work is needed to determine the biochemical function of AGO6 in TGS and its relationship with other AGO family members. Notwithstanding, our results here provide strong evidence that AGO6 is important for the accumulation of siRNAs, DNA methylation and TGS at specific loci.

Materials and methods

Plant materials, mutant isolation and gene cloning

Unless specified otherwise, WT in this study refers to the C24 ecotype carrying a firefly luciferase reporter gene driven by the *RD29A* promoter (C24 *RD29A-LUC*) (Ishitani *et al*, 1997). A T-DNA insertion population in the *ros1-1* background of *Arabidopsis thaliana* was generated as described (Kapoor *et al*, 2005). T2 seedlings were screened for *ros1* suppressors on the basis of luminescence emission and kanamycin resistance. Luminescence imaging was carried out as described (Ishitani *et al*, 1997; Kapoor *et al*, 2005). T-DNA insertion sites were determined by using TAIL-PCR (Liu *et al*, 1995).

Total RNA and small RNA extractions and Northern blot analysis

Total RNA was extracted from 15-day-old seedlings by using 4 M guanidine thiocyanate (GT) extraction solution (4 M GT, 25 mM sodium citrate, 0.5% sarcosyl and 0.1 M mercaptoethanol). Briefly, 1–2 g of fresh material was ground in liquid N_2 and powder was decanted into a 10 ml polypropylene tube that contained 3 ml cold 4 M GT solution. After shaking, 0.3 ml of 2 M NaAc (pH 5.0), 3 ml of acid phenol and 1 ml of chloroform were added in this order and mixed. After the mixture was centrifuged at 9000 r.p.m. for 12 min at 4°C, the supernatant was transferred to a new tube, 2 volumes of 100% ethanol was added and precipitated at −70°C for 1–1.5 h. The pellet was centrifuged at 6000 r.p.m. for 10 min, and suspended in 1 ml of 4 M LiCl. Then the tube was centrifuged at 13 000 r.p.m. for 12 min at 4°C, and the supernatant (containing small size RNAs) was transferred into a new 1.5 ml tube for later siRNA purification. The pellet (containing large size RNAs) was dissolved in 0.5 ml of DEPC-treated water and extracted with 0.5 volume of acid phenol and 0.5 volume of chloroform. The supernatant was transferred into a new tube after centrifuging at 13 000 r.p.m. for 10 min and then precipitated at −20°C for overnight by adding 0.1 volume of 3 M NaAc (pH 5.0) and 2 volumes of 100% ethanol. The pellet was centrifuged at 13 000 r.p.m. for 15 min and resuspended in RNase-free water.

For siRNA purification, the supernatant containing small size RNAs in 4 M LiCl was precipitated at −70°C for overnight by adding 0.1 volume of 3 M NaAc and equal volume of isopropanol. After being centrifuged at 13 000 r.p.m. for 20 min, the pellet was dried and dissolved in 500 μl of DEPC-treated water, and then extracted with 0.5 volume of acid phenol and 0.5 volume of chloroform. After centrifuging at 13 000 r.p.m. for 12 min, the supernatant was transferred to a new tube and precipitated at 4°C for 30 min after an equal volume of precipitate solution (1 M NaCl, 20% PEG8000) was added. After centrifuging at 13 000 r.p.m. for 10 min, the supernatant was transferred to a new tube, and precipitated at −70°C for overnight by adding 0.1 volume of NaAc (pH 5.0) and equal volume of isopropanol. The pellet was centrifuged at 13 000 r.p.m. for 20 min and resuspended in RNase-free water.

For analysis of mRNAs, 20 μg of total RNA was resolved on 1.2% denaturing agarose gel (MOPS-formaldehyde) and blotted onto nylon membrane. For small RNA analysis, 80 μg of small RNA was resolved on a 17% polyacrylamide-7 M urea gel and transferred electrophoretically to Hybond N_membranes (Amersham, Piscataway). PerfectHyb Plus Hybridization Buffer (Sigma, H7033-125ML) was used for mRNAs and siRNAs hybridizations according to the manufacture's instructions. Probes used for mRNA Northern blot were according to Kapoor *et al* (2005). The siRNA oligos for siRNA Northern blots for *siRNA02, siRNA1003, AtSN1* (Cao *et al*, 2003; Zilberman *et al*, 2004), *AtREP2, SIMPLEHAT2, MEA-ISR* (Qi *et al*, 2006), *mir165, miR172* and U6 are listed in Supplementary Table 1. Small RNA Northern blots were quantified after removing background: $(\text{small RNA}_{(X)}/\text{U6}_{(X)})/(\text{small RNA}_{(\text{Col-0 or WT})}/\text{U6}_{(\text{Col-0 or WT})})$, here X indicates different samples, such as Col-0, *dcl3-7, rdr2-1, ago6-2,* WT and *ago6-1.* Col-0 was control for *dcl3-7, rdr2-1, ago6-2* and WT was control for *ago6-1*.

PCR-based AtSN1 cytosine methylation assay

PCR-based *AtSN1* methylation assay was performed according to Onodera *et al* (2005). Briefly, after purified DNA was digested with *Hae*III (or undigested for controls), DNA was used for each PCR. PCR conditions were 2 min at 94°C, followed by 35 cycles of 94°C for 30 s, 53°C for 30 s and 72°C for 30 s. Primer for *AtSN1* and *At2g19920* are listed in Supplementary Table 1.

DNA bisulfite sequencing analysis

DNA bisulfite sequencing was performed according to Frommer *et al* (1992) and Kapoor *et al* (2005) with slight modifications. Briefly, after digestion with *Eco*RV and purification by phenol: chloroform (1:1), 14 μl (500–800 ng) of genomic DNA was denatured at 94°C for 5 min, and then 0.84 μl of fresh 5 N NaOH was added, followed by incubation at 39°C for 20 min. A total of 120 μl of DNA sodium bisulfite treatment mixture, containing 102 μl of fresh 40.5% sodium bisulfite (pH 5.0, adjusted with 10 N NaOH) (Sigma, S-9000-500G), 3 μl of fresh 20 mM hydroquinone (Sigma, H9003-100G) and 14.84 μl of denatured DNA was prepared and subjected to PCR under the following conditions: first four cycles: 55°C for 3 h and 94°C for 5 min, followed by one cycle at 55°C for 3 h, and finally incubated at 4°C. Sodium bisulfite-treated DNA was purified with Wizard DNA Clean-up system (Promega, #A 7280) according to the manufacturer's instruction, and at the last step, DNA was dissolved with 200 μl of H_2O at 65°C. The recollected DNA was incubated at 37°C for 20 min after 13 μl of 5 N NaOH was added, followed by precipitation at −80°C overnight by adding 210 μl of NH_4Ac (pH 7.0) and 1200 μl of 100% ethanol. After centrifuging at 13 000 r.p.m. for 20 min, DNA was dissolving in 100 μl of water. PCR was performed with LA *Taq* polymerase (TaKaRa) with

the following program: PCR mixture was first denatured at 94°C for 5 min, followed by 50 cycles: 94°C for 15 s, 54°C for 15 s and 72°C for 30 s, and last cycle at 72°C extended for 10 min. PCR products were cloned with pGEM-T Easy Vector System I (Promega, no. A1360) and transfected into DH10B competent cells. For each sample, at least 18 clones were sequenced.

Immunostaining

A construct containing *AGO6* genomic DNA fused with *MYC* tag driven by endogenous *AGO6* promoter was inserted into the pCAMBIA 1305.1 vector. The construct was transformed into *ros1-1ago6-1* double-mutant plants, and the transgene was shown to restore the bioluminescence phenotype of *ros1-1ago6-1* plants to that of *ros1-1*. The T2 plants were subjected to immunostaining analysis. Nuclei were prepared according to Bowler *et al* (2004), and stained with monoclonal anti-MYC antibodies (Clontech, 1:200 dilution). The staining patterns were visualized via Alexa Fluor 488-conjugated secondary antibodies (Molecular Probe; 1:2000 dilution) under a Leica fluorescence microscope equipped with proper filters.

Transgenic plants

AGO6 genomic DNA was amplified from BAC clone, T21L14, with Platium *pfx* DNA polymerase (Invitrogen, no. 11708-013) with forward primer, AGO6-gDNA-5F and reverse primer, AGO6-gDNA-3R, and PCR product was cloned into the *Sac*I and *Hind*III sites of pCAMBIA 1305.1. *AGO-MYC* construct was constructed by inserting AGO6-MYC-tag into *pCAMBIA 1305.1*. *AGO6* cDNA containing the entire open reading frame was amplified by RT–PCR with forward primer, AGO6-cDNA-5F, and reverse primer, AGO6-cDNA-3R. The amplified product was cloned into pDONR207 (Invitrogen) with BP clonase (Invitrogen) following the manufacturer's instructions. pEearlyGate104 was used for construct to express YFP-AGO6 fusion protein in *Arabidopsis*. For AGO6 promoter–GUS construct, *AGO6* promoter was amplified from BAC clone, T21L14, with Platium *pfx* DNA polymerase (Invitrogen, no. 11708-013) with forward primer, pAGO6-5F, and reverse primer, pAGO6-3R and the PCR product was cloned into the *Pst*I and *Eco*RI sites of pCAMBIA 1391Z. The constructs were introduced into *Arabidopsis* through floral-dip transformation with *Agrobacterium* GV301. Transgenic lines were selected based on hygromycine resistance for *AGO6* complementation, and Basta resistance for *YFP-AGO6* and *AGO6* promoter–*GUS* constructs. For GUS staining, transgenic plants were incubated overnight at 37°C in GUS staining buffer (3 mM x-Gluc, 0.1 M sodium-phosphate buffer, pH 7, 0.1% Triton X-100 and, 8 mM β-mercaptoethanol), and then chlorophyll was removed by incubating the tissue in 80% EtOH at 80°C.

Reverse transcription–PCR

A total of 34 μl of the mixture including 5 μg of total RNA, 2 μl of 100 mM poly(dT)18 and 27 μl DEPC-treated water was denatured at 65°C for 10 min, and then annealed at room temperature for 10 min. For RT, the annealed mixture was mixed with the following components: 5 μl 10 × RT buffer, 5 μl 10 mM dNTP, 4 μl 0.1 M DTT, 1 μl reverse transcriptase (Promega), 1 μl RNase inhibitor (TaKaRa) and then incubated at 37°C for 1 h, followed by incubation at 70°C for 10 min. *TUB8* was used as loading control.

Supplementary data

Supplementary data are available at *The EMBO Journal* Online (http://www.embojournal.org).

Acknowledgements

This work was supported by a National Institutes of Health grant R01GM070795 to J-K Zhu.

References

Adenot X, Elmayan T, Lauressergues D, Boutet S, Bouche N, Gasciolli V, Vaucheret H (2006) DRB4-dependent TAS3 trans-acting siRNAs control leaf morphology through AGO7. *Curr Biol* **16:** 927–932

Agarwal M, Hao Y, Kapoor A, Dong CH, Fujii H, Zheng X, Zhu JK (2006) A R2R3-type myb transcription factor is involved in the cold-regulation of CBF genes and in acquired freezing tolerance. *J Biol Chem* **281:** 37636–37645

Bartel DP (2004) MicroRNAs: genomics, biogenesis, mechanism, and function. *Cell* **116:** 281–297

Baulcombe D (2004) RNA silencing in plants. *Nature* **431:** 356–363

Baumberger N, Baulcombe DC (2005) Arabidopsis Argonaute1 is an RNA Slicer that selectively recruits microRNAs and short interfering RNAs. *Proc Natl Acad Sci USA* **102:** 11928–11933

Bender J (2004) Chromatin-based silencing mechanisms. *Curr Opin Plant Biol* **7:** 521–526

Bohmert K, Camus I, Bellini C, Bouchez D, Caboche M, Benning C (1998) AGO1 defines a novel locus of *Arabidopsis* controlling leaf development. *EMBO J* **17:** 170–180

Bouche N, Lauressergues D, Gasciolli V, Vaucheret H (2006) An antagonistic function for *Arabidopsis* DCL2 in development and a new function for DCL4 in generating viral siRNAs. *EMBO J* **25:** 3347–3356

Bowler C, Benvenuto G, Laflamme P, Molino D, Probst AV, Tariq M, Paszkowski J (2004) Chromatin techniques for plant cells. *Plant J* **39:** 776–789

Brodersen P, Voinnet O (2006) The diversity of RNA silencing pathways in plants. *Trends Genet* **22:** 268–280

Cao X, Aufsatz W, Zilberman D, Mette MF, Huang MS, Matzke M, Jacobsen SE (2003) Role of the DRM and CMT3 methyltransferases in RNA-directed DNA methylation. *Curr Biol* **13:** 2212–2217

Carrington JC, Ambros V (2003) Role of microRNAs in plant and animal development. *Science* **301:** 336–338

Chan SW, Henderson IR, Jacobsen SE (2005) Gardening the genome: DNA methylation in *Arabidopsis thaliana*. *Nat Rev Genet* **6:** 351–360

Fahlgren N, Montgomery TA, Howell MD, Allen E, Dvorak SK, Alexander AL, Carrington JC (2006) Regulation of auxin response factor3 by TAS3 ta-siRNA affects developmental timing and patterning in *Arabidopsis*. *Curr Biol* **16:** 939–944

Frommer M, McDonald LE, Millar DS, Collis CM, Watt F, Grigg GW, Molloy PL, Paul CL (1992) A genomic sequencing protocol that yields a positive display of 5-methylcytosine residues in individual DNA strands. *Proc Natl Acad Sci USA* **89:** 1827–1831

Garcia D, Collier SA, Byrne ME, Martienssen RA (2006) Specification of leaf polarity in *Arabidopsis* via the trans-acting siRNA pathway. *Curr Biol* **16:** 933–938

Gong Z, Morales-Ruiz T, Ariza RR, Roldan-Arjona T, David L, Zhu JK (2002) ROS1, a repressor of transcriptional gene silencing in *Arabidopsis*, encodes a DNA glycosylase/lyase. *Cell* **111:** 803–814

He L, Hannon GJ (2004) MicroRNAs: small RNAs with a big role in gene regulation. *Nat Rev Genet* **5:** 522–531

Hunter C, Sun H, Poethig RS (2003) The *Arabidopsis* heterochronic gene ZIPPY is an Argonaute family member. *Curr Biol* **13:** 1734–1739

Hunter C, Willmann MR, Wu G, Yoshikawa M, de la Luz Gutierrez-Nava M, Poethig SR (2006) Trans-acting siRNA-mediated repression of ETTIN and ARF4 regulates heteroblasty in *Arabidopsis*. *Development* **133:** 2973–2981

Ishitani M, Xiong L, Stevenson B, Zhu JK (1997) Genetic analysis of osmotic and cold stress signal transduction in *Arabidopsis*: interactions and convergence of abscisic acid-dependent and abscisic acid-independent pathways. *Plant Cell* **9:** 1935–1949

Kapoor A, Agarwal M, Andreucci A, Zheng X, Gong Z, Hasegawa PM, Bressan RA, Zhu JK (2005) Mutations in a conserved replication protein suppress transcriptional gene silencing in a DNA-methylation-independent manner in *Arabidopsis*. *Curr Biol* **15:** 1912–1918

Li CF, Pontes O, El-Shami M, Henderson IR, Bernatavichute YV, Chan SW, Lagrange T, Pikaard CS, Jacobsen SE (2006) An Argonaute4-containing nuclear processing center colocalized with Cajal bodies in *Arabidopsis thaliana*. *Cell* **126:** 93–106

Liu J, Carmell MA, Rivas FV, Marsden CG, Thomson JM, Song JJ, Hammond SM, Joshua-Tor L, Hannon GJ (2004) Argonaute2 is the catalytic engine of mammalian RNAi. *Science* **305:** 1437–1441

Liu YG, Mitsukawa N, Oosumi T, Whittier RF (1995) Efficient isolation and mapping of *Arabidopsis thaliana* T-DNA insert

junctions by thermal asymmetric interlaced PCR. *Plant J* **8:** 457–463

Lynn K, Fernandez A, Aida M, Sedbrook J, Tasaka M, Masson P, Barton MK (1999) The PINHEAD/ZWILLE gene acts pleiotropically in *Arabidopsis* development and has overlapping functions with the ARGONAUTE1 gene. *Development* **126:** 469–481

Matzke MA, Birchler JA (2005) RNAi-mediated pathways in the nucleus. *Nat Rev Genet* **6:** 24–35

Meister G, Landthaler M, Patkaniowska A, Dorsett Y, Teng G, Tuschl T (2004) Human Argonaute2 mediates RNA cleavage targeted by miRNAs and siRNAs. *Mol Cell* **15:** 185–197

Meister G, Tuschl T (2004) Mechanisms of gene silencing by double-stranded RNA. *Nature* **431:** 343–349

Mello CC, Conte Jr D (2004) Revealing the world of RNA interference. *Nature* **431:** 338–342

Miyoshi K, Tsukumo H, Nagami T, Siomi H, Siomi MC (2005) Slicer function of *Drosophila* Argonautes and its involvement in RISC formation. *Genes Dev* **19:** 2837–2848

Moissiard G, Voinnet O (2006) RNA silencing of host transcripts by cauliflower mosaic virus requires coordinated action of the four *Arabidopsis* Dicer-like proteins. *Proc Natl Acad Sci USA* **103:** 19593–19598

Morel JB, Godon C, Mourrain P, Beclin C, Boutet S, Feuerbach F, Proux F, Vaucheret H (2002) Fertile hypomorphic Argonaute (ago1) mutants impaired in post-transcriptional gene silencing and virus resistance. *Plant Cell* **14:** 629–639

Morris KV (2005) siRNA-mediated transcriptional gene silencing: the potential mechanism and a possible role in the histone code. *Cell Mol Life Sci* **62:** 3057–3066

Moussian B, Schoof H, Haecker A, Jurgens G, Laux T (1998) Role of the ZWILLE gene in the regulation of central shoot meristem cell fate during *Arabidopsis* embryogenesis. *EMBO J* **17:** 1799–1809

Onodera Y, Haag JR, Ream T, Nunes PC, Pontes O, Pikaard CS (2005) Plant nuclear RNA polymerase IV mediates siRNA and DNA methylation-dependent heterochromatin formation. *Cell* **120:** 613–622

Pal-Bhadra M, Bhadra U, Birchler JA (2002) RNAi related mechanisms affect both transcriptional and posttranscriptional transgene silencing in *Drosophila*. *Mol Cell* **9:** 315–327

Pontes O, Li CF, Nunes PC, Haag J, Ream T, Vitins A, Jacobsen SE, Pikaard CS (2006) The *Arabidopsis* chromatin-modifying nuclear siRNA pathway involves a nucleolar RNA processing center. *Cell* **126:** 79–92

Qi Y, Denli AM, Hannon GJ (2005) Biochemical specialization within *Arabidopsis* RNA silencing pathways. *Mol Cell* **19:** 421–428

Qi Y, He X, Wang XJ, Kohany O, Jurka J, Hannon GJ (2006) Distinct catalytic and non-catalytic roles of Argonaute4 in RNA-directed DNA methylation. *Nature* **443:** 1008–1012

Rand TA, Petersen S, Du F, Wang X (2005) Argonaute2 cleaves the anti-guide strand of siRNA during RISC activation. *Cell* **123:** 621–629

Ronemus M, Vaughn MW, Martienssen RA (2006) MicroRNA-Targeted and small interfering RNA-mediated mRNA degradation is regulated by Argonaute, Dicer, and RNA-dependent RNA polymerase in *Arabidopsis*. *Plant Cell* **18:** 1559–1574

Sigova A, Rhind N, Zamore PD (2004) A single Argonaute protein mediates both transcriptional and posttranscriptional silencing in *Schizosaccharomyces pombe*. *Genes Dev* **18:** 2359–2367

Tabara H, Sarkissian M, Kelly WG, Fleenor J, Grishok A, Timmons L, Fire A, Mello CC (1999) The rde-1 gene, RNA interference, and transposon silencing in *C. elegans*. *Cell* **99:** 123–132

Tang G (2005) siRNA and miRNA: an insight into RISCs. *Trends Biochem Sci* **30:** 106–114

Tijsterman M, Okihara KL, Thijssen K, Plasterk RH (2002) PPW-1, a PAZ/PIWI protein required for efficient germline RNAi, is defective in a natural isolate of *C. elegans*. *Curr Biol* **12:** 1535–1540

Vaucheret H, Vazquez F, Crete P, Bartel DP (2004) The action of Argonaute1 in the miRNA pathway and its regulation by the miRNA pathway are crucial for plant development. *Genes Dev* **18:** 1187–1197

Verdel A, Moazed D (2005) RNAi-directed assembly of heterochromatin in fission yeast. *FEBS Lett* **579:** 5872–5878

Wassenegger M (2005) The role of the RNAi machinery in heterochromatin formation. *Cell* **122:** 13–16

Yigit E, Batista PJ, Bei Y, Pang KM, Chen CC, Tolia NH, Joshua-Tor L, Mitani S, Simard MJ, Mello CC (2006) Analysis of the *C. elegans* Argonaute family reveals that distinct Argonautes act sequentially during RNAi. *Cell* **127:** 747–757

Zhang X, Yuan YR, Pei Y, Lin SS, Tuschl T, Patel DJ, Chua NH (2006) Cucumber mosaic virus-encoded 2b suppressor inhibits *Arabidopsis* Argonaute1 cleavage activity to counter plant defense. *Genes Dev* **20:** 3255–3268

Zilberman D, Cao X, Jacobsen SE (2003) Argonaute4 control of locus-specific siRNA accumulation and DNA and histone methylation. *Science* **299:** 716–719

Zilberman D, Cao X, Johansen LK, Xie Z, Carrington JC, Jacobsen SE (2004) Role of Arabidopsis Argonaute4 in RNA-directed DNA methylation triggered by inverted repeats. *Curr Biol* **14:** 1214–1220